Published in final edited form as:
J Comp Neurol. 2008 October 10; 510(5): 475–483. doi:10.1002/cne.21800.

Sensory-Dependent Asymmetry for a Urine-Responsive Olfactory Bulb Glomerulus

Anthony M. Oliva[1], **Kevin R. Jones**[2], and **Diego Restrepo**[1]

[1]Department of Cell and Developmental Biology, Neuroscience Program and Rocky Mountain Taste and Smell Center, University of Colorado Denver, School of Medicine, MS 8108 Box 6511, Aurora, CO 80045

[2]Department of Molecular, Cellular, and Developmental Biology, University of Colorado, Boulder, Colorado 80309

Abstract

An unusual property of the olfactory system is that sensory input at the level of the first synapse in the olfactory bulb takes place at two mirror image glomerular maps that appear identical across the axis of symmetry. It is puzzling how two identical odor maps would contribute to sensory function. The functional units in these maps are the glomeruli, ovoid neuropil structures formed by axons from olfactory sensory neurons expressing the same olfactory receptor. Here we find that the genetically identified P2 glomeruli are asymmetric across the axis of symmetry in terms of responsiveness to urine volatiles and neuroanatomical structure. Furthermore, P2 asymmetry is modified by sensory deprivation and abolished by decreased BDNF levels. Thus, while mirror odor maps show symmetry at the macroscopic level in maps encompassing the entire surface of the olfactory bulb, they display asymmetry at the level of the single glomerulus.

Keywords

Olfactory bulb; glomerulus; BDNF; sensory deprivation; naris occlusion

Introduction

Mice have a remarkable ability of detecting subtle differences in odor quality (Rinberg et al., 2006;Uchida and Mainen, 2003;Linster et al., 2001). For example urine volatiles from mice differing at a single gene in the major histocompatibility complex (MHC) can be discriminated by smell and elicit distinct activity patterns in the mouse olfactory bulb (Schaefer et al., 2002). This exquisite ability to differentiate between subtle dissimilarities in volatile odor quality is accomplished by expression of a large array of odorant receptors (ORs), ~1000 in the mouse, in olfactory sensory neurons (OSNs) residing in the main olfactory epithelium (MOE) (Buck and Axel, 1991;Buck, 2005). Thousands of axons from OSNs expressing the same OR project to the main olfactory bulb (MOB) and synapse with mitral/tufted cells in a few discrete ovoid neuropil structures called glomeruli thought to be functional units of activity analogous to cortical barrels in somatosensory cortex (Mombaerts et al., 1996;Treloar et al., 2002). Because of the exclusive targeting of each glomerulus by OSNs expressing a particular OR odor quality is thought to be encoded by the pattern of activity of glomeruli in the MOB. Indeed, odor-elicited spatial (and temporal)

Correspondence to be sent to: Diego Restrepo, University of Colorado Denver, Anschutz Medical Center, DEPT CDB, Mail Stop 8108, PO BOX 6511, Aurora CO 80045, work: (303) 724-3405, fax: (303) 724-3420, diego.restrepo@uchsc.edu.
Associate Editor: Joseph L. Price

activity patterns of glomerular activation (odor maps) differ among a wide variety of odors (Johnson and Leon, 2007;Spors et al., 2006;Royet et al., 1988;Wachowiak and Cohen, 2001;Friedrich and Korsching, 1998;Sharp et al., 1977;Mori et al., 2006;Rubin and Katz, 1999;Nagao et al., 2000;Schaefer et al., 2002).

An unusual feature of the projection of axons from the epithelium to the bulb is that patterns of projection by OSNs bearing a particular receptor are bilaterally symmetric resulting in two mirror-image OSN axon projection maps (glomerular maps) (Mombaerts et al., 1996;Lodovichi et al., 2003). In accordance to the mirror-image arrangement of the glomerular maps, the odor maps display the same mirror-image symmetry about an axis separating the medial and lateral MOB (Mori et al., 2006;Johnson and Leon, 2007). Such an arrangement of the input into two mirror odor maps is curious, and the role for this dual map in olfaction is not understood. An intrabulbar circuit connects the two mirror glomerular columns found in each of the mirror maps (Marks et al., 2006;Lodovichi et al., 2003). Presumably, the activity in the two glomerular response maps is contrasted through this intrabulbar circuit and dual maps exist to provide differential input that can convey additional information to the olfactory bulb. But, how does this happen if the information represented in the two maps is the same? Here we report on experiments designed to determine whether the genetically identified glomerulus P2 is functionally and structurally asymmetric across the mirror symmetry axis, and what factors influence structural asymmetry at the level of the individual glomerulus.

Materials and Methods

Animals

All experiments were performed under protocols approved by the Animal Care and Use Committee of the University of Colorado at Denver and Health Sciences Center. Adult male P2-IRES-tauGFP mice 12–16 weeks of age (Mombaerts et al., 1996) and adult male and female P2-IRES-tauGFP/BDNF-LacZ mice 12–16 weeks of age were used for this study. To generate P2-IRES-tauGFP/BDNF-LacZ mice, heterozygous BDNF-LacZ males (Bennett et al., 1999) were mated with homozygous P2-IRES-tauGFP females (Mombaerts et al., 1996). It is important to note that the BDNF-LacZ mutation knocks out the BDNF allele and that a homozygous BDNF-LacZ mouse fails to survive much beyond 10 days. Unless otherwise noted, all mice were group-housed in Static Micro-BARRIER cages (MBS75JHT) from Allentown Inc. with food and water available *ad libitum*.

Odor Exposure

Urine (H-2b) was collected at 8 a.m. from five unrelated adult male C57/BL6 mice (between 12 and 24 weeks of age), pooled and diluted to 20% vol/vol in water (Schaefer et al., 2002). Odor exposure was performed as in our previous experiments (Lin et al., 2004). Briefly, test animals were placed in a 500 cubic centimeter Plexiglas chamber supplied with humidified fresh air flowing continuously at 300 ml/min. A manual 3-way valve controlled the delivery of either a fresh air or urine volatile-containing air stream at 300 ml/min to the Plexiglas chamber. All test mice were exposed to fresh air for 90 minutes prior to exposure to either fresh air or urine, thus allowing the animal to acclimate to the chamber and for Fos expression due to cage and self odors to decrease. Odor exposure occurred intermittently to minimize adaptation effects where either urine or fresh air was presented over six intervals for 2 minutes and fresh air for 3 minutes over a 30 minute stimulus period. Mice remained in the chamber for 60 additional minutes then were sacrificed.

Naris Occlusion

Mice were born and raised in highly ventilated Micro-VENT cages (MBS75JHTMV) from Allentown Inc until the time of surgery. In these ventilated cages air was exchanged by addition and removal of HEPA-filtered fresh air at a rate of one volume per minute. The surgical procedure was adapted from Baker et al. (1993). Twelve-week old adult mice were anesthetized with ketamine-xylazine (100 μg/g-20 μg/g bodyweight). The left or right naris was cauterized with an electrical cautery tool (Aaron Medical Industries, St. Petersburg, FL) in seven mice. In six other mice, sham surgery was performed where a portion of the skin on the nose adjacent to the naris on the left or right side was cauterized. After surgery, ointment and infant Tylenol were administered to alleviate pain. These mice were subsequently group-housed in the Static Micro-BARRIER cages (MBS75JHT). After four weeks the mice were sacrificed after testing for complete naris occlusion by showing that breathing does not result in flow of air and formation of a bubble when soapy water is placed directly on the cauterized naris.

Tissue Preparation

All mice used in this study were anesthetized with 20% chlorohydrate, perfused transcardially with 0.1M phosphate-buffered saline (PBS) (137mM NaCl, 2.7 mM KCl, 4.3 mM $Na_2HPO_47H_2O$, and 1.4 mM KH_2PO_4, pH 7.4) and heparin, followed by fixative. The fixative used for Fos immunohistochemistry was 0.1M PBS containing 3% paraformaldehyde, 0.019M L-lysine monohydrochloride, and 0.23% sodium m-periodate. All other brains were fixed with 0.1M PBS containing 4% paraformaldehyde. The brains were then harvested and post-fixed for 2 hours on ice before cryoprotection by incubation in 0.1M PBS with 30% sucrose overnight at 4°C. The brains were placed in a positional mold and cut through the forebrain at an angle perpendicular to the lateral olfactory tract (Schaefer et al., 2001). The remaining forebrain was then mounted directly onto a chuck and frozen with O.C.T. compound (Tissue-Tek®, USA) with the olfactory bulbs at the top and with the lateral olfactory tract perpendicular to the plane of section.

Immunohistochemistry and Antibody Characterization

Olfactory bulbs were cut coronally at 18 μm and collected onto glass slides. Sections were rinsed in 0.1M PBS and incubated in blocking solution containing 2% normal donkey serum, 0.3% Triton X-100, and 1% bovine serum albumin in 0.1M PBS for 1.5 hr. To label Fos protein, the sections were incubated with polyclonal rabbit antibody (Calbiochem Cat. No. PC05T) at 1:1,000 dilution in blocking solution for 72 hr at 4°C. This Fos Ab is made in rabbits against the synthetic peptide SGFNADYEASSSRC corresponding to amino acids 4–17 of human c-fos. The Ab recognizes a single 50–62 kDa Fos protein in a Western blot. As a control for specificity the immunolabeling with the Fos Ab decreased markedly upon processing of olfactory bulb from mice exposed to fresh air. To label tyrosine hydroxylase (TH) protein, the sections were incubated with polyclonal rabbit antibody (Calbiochem Cat. No. 657012) at 1:2,000 dilution in blocking solution. This antibody was raised against purified, SDS-denatured rat pheochromocytoma tyrosine hydroxylase. As expected (Baker et al., 1993), this antibody labels a subset of periglomerular cells, and its immunoreactivity decreases markedly after naris occlusion for a month. To label β-galactosidase protein, the sections were incubated with polyclonal guinea pig antibody (Yee et al. 2003) at 1:1,000 dilution in blocking solution for 48 hr at 4°C. This antibody was made against β-galactosidase (Sigma, St. Louis). We performed a thorough set of control experiments where we showed in mice that do not express β-galactosidase that the antibody did not mediate immunoreactivity in the olfactory bulb and olfactory epithelium (Clevenger et al., 2008). Sections were then incubated with Alexa 568 secondary antibody (Molecular Probes, Eugene, OR) and subsequently counterstained with DAPI, a nuclear stain. Slides were then coverslipped using Fluormount.

Imaging and Cell counts

For cell counts sections were photographed on a Nikon Eclipse E600 microscope (Tokyo, Japan) with a 40X objective using a Spot RT camera and software. A P2 glomerulus was defined as a region of GFP-labeled neuropil bounded by DAPI stained juxtaglomerular cells. Fos-like IR or TH-IR and DAPI stained juxtaglomerular cells that were immediately adjacent to the P2 glomerulus (less than 2 nuclei widths from the outer boundary of the P2 axon fibers within the glomerulus) were counted in serial sections using the physical dissector method (Howard 1998). A cell was considered immunoreactive if the intensity exceeded by 2 times the standard deviation the intensity of staining in the middle of the glomerulus. In the counts of the number of juxtaglomerular cells we do not differentiate between periglomerular cells and external tufted cells. However, because the number of periglomerular cells is much larger than the number of external tufted cells, the numbers reported likely represent mostly the number of periglomerular cells. The percent of total number of Fos-like IR cells to total number of DAPI stained cells surrounding P2 glomeruli was used for statistical analysis. Fluorescent micrographs shown in Figure 2–Figure 5 were acquired with an Olympus BX50 Fluoview confocal laser scanning microscope. Images were taken using a high magnification 60X oil immersion lens.

Within an experiment all images were acquired under the same exposure conditions. To create the figures the images in all panels were modified to the same extent by changing brightness using the levels function in Adobe Photoshop.

Volume Measurements and Statistics

We used Image J software to calculate cross-sectional area of a particular glomerulus in a section and then calculated the volume of that glomerulus by summing the cross-sectional areas and multiplying that sum by the thickness of a section (18 μm).

Data obtained from the P2 glomerular and domain volume measurements, the number of P2 glomeruli in a given domain, the number of JG cells per P2 glomerulus, and the percentage of Fos-IR and TH-IR JG cells were compared statistically using SAS software. Briefly, the statistical significance of differences for these variables for different effects was determined using a mixed effects analysis of variance (Searle et al., 1992). Mouse was considered a random effect, while the sex and domains (medial or lateral) were considered fixed effects. The total number of JG cells was entered as a covariate for the statistical analysis of the data in Figure 3H and Figure 4C. The mixed ANOVA was implemented by the SAS procedure MIXED (SAS Institute Inc., 2004). A post-hoc Tukey-Kramer test then generated P values for all comparisons. Graphic visualization of data was performed using Microcal Origin 7.0 to plot data using means and standard error.

Results

Neuroanatomical Features of P2 Glomeruli Show Asymmetry across Domains

In comparing previous studies, we made the observation that odor maps for urine may not be symmetrical as judged by using the location of genetically identified glomeruli as fiduciary marks for the mirror image maps (Salcedo et al., 2005). Specifically, urine from mice differing in their genotype at the MHC (H-2k and H-2b haplotypes), appear to elicit symmetrical and asymmetrical odor maps respectively (Salcedo et al., 2005). Here we focused our attention on a genetically identified glomerulus, the glomerulus targeted by OSNs expressing the P2 odor receptor because these glomeruli are located in regions of the mirror image odor maps that show distinct asymmetry for H-2b urine (more glomeruli express urine-induced c-fos expression in the medial domain). We surveyed the neuroanatomical characteristics of the P2 glomeruli in genetically altered mice expressing

tauGFP in P2 OSNs. We compared the neuroanatomical features of the P2 glomeruli found in mirror locations across the symmetry line of the odor map. In the rest of the manuscript we refer to these two locations as the medial and lateral domains of the glomerular map.

Strikingly, we noticed differences reproducible from mouse to mouse in the number and volume of P2 glomeruli across medial and lateral domains encompassing the mirror image glomerular maps. Figure 1A shows fluorescent micrographs of serial sections through a single glomerulus where DAPI-stained juxtaglomerular cells (JG cells) that surround P2 glomeruli are shown in magenta, and the axons of the P2 neurons labeled by the genetic marker tauGFP are shown in green. We find the medial glomeruli are significantly larger compared to lateral glomeruli: 697,751 ± 49,801 μm^3 and 503,110 ± 45,890 μm^3, respectively ($F_{1,38}$=8.09, P=0.0071) (Figure 1B). In contrast, when we summed the volume of all glomeruli in each domain (the P2 domain volume) there was no difference between the lateral and medial aspects ($F_{1,23}$=0.12, P=0.733) (Figure 1C). The lack of a difference in domain volume is due to the fact that the number of P2 glomeruli in each domain differed significantly. Specifically, there are more P2 glomeruli in the lateral compared to the medial aspect (1.69 ± 0.12 lateral glomeruli and 1.25 ± 0.11 medial glomeruli, $F_{1,23}$=7.14, P=0.0136) (Figure 1F). This suggests that, while on the medial side the glomeruli are able to coalesce to a single glomerulus, the axons on the lateral side have a tendency to form smaller multiple glomeruli.

To begin to determine the factors contributing to asymmetry in P2 glomerular volume we determined whether the number of JG cells surrounding P2 glomeruli differed between lateral and medial glomeruli. We counted all DAPI-labeled nuclei immediately adjacent to the P2 glomeruli and found significant differences in the number of total JG cells surrounding the lateral and medial P2 glomeruli: 822.9 ± 69.9 and 1040 ± 55.4, respectively ($F_{1,38}$=5.30, P=0.0269) (Figure 1D). These results do correlate with the P2 glomerular volume findings thus the total number of JG cells may be a factor dictating glomerular volume. Consistent with the P2 domain volume findings, the total number of JG cells per P2 domain did not differ ($F_{1,23}$=0.62, P=0.4388) (Figure 1E).

Response of P2 Glomeruli to Urine –Measured with Fos Immunoreactivity–is Asymmetric Across Domains

Our previous studies showed that P2 was located in areas of the bulb that responded asymmetrically to mouse urine raising the question whether P2 itself responds asymmetrically. To test whether the JG cells surrounding P2 glomeruli are responsive to urine, male mice were exposed to urine from C57BL/6 male mice (an H-2b haplotype in the MHC) or fresh air and we determined the number of cells expressing the immediate early gene product Fos, a protein known to be upregulated in JG cells surrounding urine odor-activated glomeruli (Schaefer et al., 2002;Salcedo et al., 2005).

We find that P2 glomeruli respond to urine as indicated by a larger percent of Fos-immunoreactive (Fos-IR) JG cells surrounding P2 glomeruli in MOBs from mice exposed to urine compared to fresh air (Figure 2). Figures 2A–F are representative laser scanning confocal micrographs of immunofluorescence for Fos in JG cells (magenta) surrounding the P2 glomeruli (tauGFP shown in green) in mice exposed to fresh air (Figure 2A–C) and urine (Figure 2D–F) and Figure 2G is a bar graph quantifying the percent of Fos-IR positive JG cells for the different domains (medial vs. lateral) and odor exposure conditions (urine vs. fresh air). A mixed effects ANOVA indicated a significant effect of odor exposure (urine vs. fresh air) on the percent of Fos-IR JG cells ($F_{1,6}$=8.46, P=0.0270) indicating that the P2 glomerulus is urine-responsive. Consistent with this premise, post hoc tests reveal a significant increase in the proportion of JG cells with Fos-like IR in mice exposed to urine compared to fresh air for both the lateral and medial glomeruli: 3.17 ± 0.31 to 0.84 ± 0.09

and 2.13 ± 0.20 to 0.74 ± 0.17 respectively (Figure 2G). In addition, and as expected from previous work in our laboratory (Schaefer et al., 2001), the urine response of glomeruli in the vicinity of P2 was asymmetric across the domains. Thus, when the mice were exposed to H-2b urine there were few glomeruli surrounded by Fos-IR cells in the vicinity of the urine-responsive lateral P2 glomerulus while there were many Fos-positive glomeruli surrounding the medial P2 glomerulus (not shown).

Interestingly, the response of P2 glomeruli, measured as the percent of Fos-IR positive JG cells, was asymmetric. Thus, a mixed effects ANOVA revealed a significant effect of the interaction between domain and odor exposure on the percent of Fos-IR positive JG cells surrounding P2 (Figure 2G, $F_{1,29}$=4.28, P=0.0475). Post-hoc tests revealed that the proportion of Fos-like IR JG cells adjacent to the P2 glomeruli was asymmetric when the medial glomeruli were compared to the lateral glomeruli only in mice exposed to urine (P=0.0042), which is not seen in the fresh air controls (P=0.9937) (Figure 2G). These data suggest that the P2 glomerulus responds asymmetrically to H-2b urine.

Asymmetry in TH Immunoreactive Juxtaglomerular Cells Surrounding P2 Glomeruli in Mice

TH expression in JG cells is well known to be dependent on previous long term odor exposure (Baker et al., 1993). The asymmetric response to urine found in the Fos-IR measurements raised the question whether long-term exposure to cage odor results in asymmetric changes in TH expression in the JG cells surrounding the P2 glomeruli. We examined whether the percent of TH-IR JG cells surrounding P2 glomeruli differed across domains. Figure 3A shows a representative laser scanning micrograph of immunofluorescence of TH in JG cells (magenta) surrounding a P2 glomerulus (tauGFP is shown in green). A one-way ANOVA indicated a significant effect of domain (lateral vs. medial) on the percent of TH-IR JG cells surrounding P2 glomeruli ($F_{1,29}$=10.44, P=0.0031) (Figure 3B). Thus, there are a significantly larger proportion of JG cells with TH-like IR in the lateral glomeruli compared to the medial glomeruli. Because TH activity is dependent on odor-induced activity in OSNs, our results suggest that P2 glomeruli are differentially affected across domains by long term cage odor exposure.

Naris Occlusion Alters Across-Domain Asymmetry of Anatomical Features of P2 Glomeruli

Previous studies indicate that activity influences the number of glomeruli formed by OSNs expressing the same olfactory receptor type (Zou et al., 2004). To test whether activity influences neuroanatomical features of P2 glomeruli we performed a unilateral naris occlusion in twelve week-old mice and determined whether sensory deprivation affects the size and number of P2 glomeruli across domains four weeks following naris occlusion. Naris occlusion had a dramatic effect on glomerular volume and the number of glomeruli per domain. Figure 4A shows representative fluorescence micrographs of DAPI counterstained JG cells (magenta) and P2 glomeruli (tauGFP in green) in the lateral and medial domains of occluded and non-occluded olfactory bulbs. A mixed effects ANOVA indicated significant effects of naris occlusion on P2 glomerular volume ($F_{1,12}$=11.52, P=0.0053) (Figure 4B), P2 domain volume ($F_{1,12}$=20.58, P=0.0007) (Figure 4C), and the number of P2 glomeruli ($F_{1,12}$=13.04, P=0.0036) (Figure 4F) of occluded vs. non-occluded bulbs. The effect on the number of glomeruli was particularly striking on the lateral domain where we could find no P2 glomeruli in several bulbs on the occluded side, a result that we never find in naive animals (Figure 4G).

In terms of asymmetry, the effects of sensory deprivation were dramatic. In those mice where the glomeruli disappeared in the lateral domain, asymmetry was extreme with a medial glomerulus and no lateral glomerulus. Interestingly, the across-domain asymmetry of

P2 was abolished. Thus the ANOVA indicated no difference between lateral and medial domain measures for all variables in either the open or occluded bulbs (P2 glomerular volume $F_{1,18}$=0.58, P=0.4544, P2 domain volume $F_{1,9}$=4.06, P=0.0747, number of P2 glomeruli $F_{1,12}$=2.09, P=0.1742). This is in contrast to mice subjected to sham naris occlusion (Figures 4D–H) whose results were identical to the experiment presented in Figure 1. For sham naris occlusion one-way ANOVA indicates significant differences across the lateral and medial domains for P2 glomerular volume ($F_{1,27}$=5.10, P=0.0323) (Figure 4D) and the number of P2 glomeruli ($F_{1,17}$=7.62,P=0.0134) (Figure 4H) but not for P2 domain volume ($F_{1,17}$=2.15,P=0.1704) (Figure 4E). These results are consistent with experiments in naive animals shown in Figure 1. It is clear that sensory deprivation alters the size and number of P2 glomeruli affecting asymmetry in a dramatic manner.

Reduced BDNF Levels Abolishes Structural Across-Domain Asymmetry in P2 Glomeruli

The experiments above show that mirror image asymmetry in P2 structure dependends on sensory experience and raise the question what molecular mechanism mediates this sensory-dependent structural asymmetry. BDNF is an attractive candidate as this neurotrophin, synthesized and released in an activity-dependent manner, is known to modulate OSN axon arborization within glomeruli (Cao et al., 2007) and because mice lacking low affinity BDNF receptors (p75NTR) display ectopic glomeruli (Tisay et al., 2000) reminiscent of the multiple P2 glomeruli we find on the medial domain of the glomerular map in P2 IRES tauGFP mice. We studied the changes in P2 glomerular structure by crossing P2 IRES tauGFP mice with mice where the coding region for BDNF had been replaced by LacZ. We used BDNF lacZ (+/−) mice because the homozygotes (−/−) die shortly after birth (Ernfors et al., 1994;Jones et al., 1994). BDNF is not expressed in olfactory sensory neurons, but is expressed in a subset of juxtaglomerular neurons surrounding the glomeruli (Figure 5A and (McLean et al., 2001)). An ANOVA indicated no significant effects of domain (lateral vs. medial) on glomerular volume ($F_{1,40}$=0.19, P=0.6686) (Figure 5B). These results demonstrate that in male mice asymmetry in glomerular volume requires 2 functional BDNF alleles. In addition, an ANOVA revealed no significant effects of domain (lateral vs. medial) on the number of glomeruli per domain ($F_{1,22}$=0.03, P=0.8551) (Figure 5C). This indicates that BDNF plays a role in setting up the structural asymmetry for P2 glomeruli across the mirror image glomerular map.

Discussion

Axons from OSNs expressing the P2 receptor typically target two glomeruli at symmetric positions within each of the two mirror-image maps of identified glomeruli found in each olfactory bulb (Mombaerts et al., 1996;Nagao et al., 2000). Here we show that despite the fact that the underlying glomerular arrangement displays mirror-image symmetry, P2 glomeruli display structural and functional asymmetries across the lateral and medial domains. Structurally, the lateral P2 glomeruli are smaller than the medial glomeruli. The difference in size may be due, in part, to differences in the number of JG cells surrounding the glomeruli. Furthermore, there are significantly more P2 glomeruli on the lateral aspect compared to the medial aspect. These asymmetries are activity-dependent and are ameliorated by decreased BDNF expression. Because BDNF modulates OSN axonal arborization (Cao et al., 2007), the difference in volume could also be influenced by differences across the mirror image glomerular map in axonal arborization. Furthermore, the responsiveness of P2 glomeruli to H-2b urine, measured by expression of Fos-like IR in surrounding JG cells, is asymmetric. Thus, we show that in male mice a larger proportion of JG cells express H-2b urine-elicited Fos-like IR in the lateral P2 glomeruli compared to the medial glomeruli. Our finding that there is an asymmetry of responses to urine odors raises

the question whether asymmetrical responses in the mirror-image odor maps in the main olfactory bulb are important for detecting subtle differences in complex odors.

The anatomical differences in P2 glomeruli could have functional consequences for odor processing. Lateral excitation through gap junctions formed by connexin 36 appears to be important in ensuring that all mitral cells innervating the same glomerulus respond to an odor feature in a concerted, synchronous manner (Christie and Westbrook, 2006;Schoppa and Westbrook, 2001). If mitral cells innervate two different P2 glomeruli within the same domain they would not communicate through gap junctions at the primary dendrite. This would presumably diminish the amplification of the sensitivity of each glomerulus to incoming sensory input mediated by lateral excitation.

H-2b Urine Elicits Asymmetric Responses –Measured with Fos IR– in P2 Glomeruli

As discussed above, genetically identified glomeruli are arranged in two mirror-image glomerular maps, one in the lateral and the other in the medial aspect of the bulb. In accordance with this mirror-image arrangement, responses of the glomeruli to monomolecular odorants show the same mirror-image symmetry (Mori et al., 2006;Johnson and Leon, 2007). In contrast, in this manuscript we find that in males the responsiveness of the P2 glomerulus to a complex odor (H-2b urine), measured by the proportion of adjacent JG cells displaying Fos-like IR, is different in lateral and medial glomeruli. Our measurements confirm previous studies that suggested the glomerular responses to some complex odors did not follow mirror-image symmetry (Schaefer et al., 2002;Xu et al., 2000). The asymmetry present in some odor maps may be due to the technique used to measure the odor-elicited activity. Thus, for example, 2-deoxyglucose uptake, which is thought to be responsive mainly to the incoming OSN activity, might be less likely to show asymmetry than a measurement such as Fos that is clearly dependent, not only on OSN input, but also on olfactory bulb processing that affects activity in periglomerular cells. Below we discuss the factors that potentially affect Fos activity differentially in the P2 glomeruli.

It is not clear why a complex odor such as H-2b urine would yield different responses on the medial and lateral sides of the bulb, but several factors likely contribute to the asymmetric response. Strotmann and co-workers have shown that the OSNs projecting their axons to the lateral and medial P2 glomeruli are located in segregated areas in the olfactory epithelium (Levai et al., 2003). Since the air flow patterns differ in these areas of the OE (Kimbell et al., 1997), and because the olfactory epithelium exhibits chromatographic features (Mozell, 1970), it is likely that the concentration of odor molecules detected by the P2 receptors differs between the medial and lateral glomeruli. Indeed, a survey of the Johnson and Leon online database (http://leonserver.bio.uci.edu/) reveals asymmetric odorant responses for a subset of stimuli. This effect of chromatographic adsorption by the olfactory epithelium would be particularly noticeable at the near threshold low volatile molecule concentrations found in urine.

Another factor likely influencing asymmetric responsiveness of JG cells associated with the medial and lateral P2 glomeruli may be intrabulbar processing. Thus, because the number of activated glomeruli in the vicinity of P2 in the medial domain is large (Schaefer et al., 2002), lateral inhibitory interactions between glomeruli (Aungst et al., 2003), or through dendrodendritic synapses between mitral cells and granule cells (Shepherd et al., 2004) could decrease the activity in JG cells in the medial P2 glomeruli. Note that lateral inhibition in the bulb does not explain why few glomeruli respond on the lateral side, this would have to be explained by lower input from OSNs caused either by decreased stimulation of OSNs by the odor due to chromatographic effects, or perhaps by general differences in presynaptic inhibition in the two domains.

Another bulbar mechanism that might affect Fos responsiveness of JG cells surrounding P2 glomeruli would be interactions across the mirror-image glomerular maps (Lodovichi et al., 2003;Marks et al., 2006). Each glomerulus has an associated “odor column”, analogous to cortical barrels or columns, that includes the mitral/tufted and juxtaglomerular cells innervating the glomerulus as well as granule cells connected to these neurons (Willhite et al., 2006). Interestingly, the external tufted cells associated with the medial P2 glomerulus project to the internal plexiform layer directly underneath the lateral P2 glomerulus where they are thought to form excitatory synapses onto granule cells within the lateral P2 odor column (there are similar projections from the lateral to the medial glomerulus). Thus the odor columns for the P2 glomeruli are specifically and reciprocally connected across the mirror-image glomerular map (Lodovichi et al., 2003) and asymmetric activation of those glomeruli could be further influenced by this intrabulbar circuit. Indeed, Katz and co-workers propose that, by analogy of some of the proposed functions of connections between mirror-image maps in visual cortex, intrabulbar connections may be involved in modulating the receptive field of tufted and/or mitral cells, which would be expected to be reflected by differential responsiveness of JG cells within the P2 odor column because JG cells receive mitral cell input (Schoppa, 2006;Shepherd et al., 2004).

Across-Domain Asymmetry in Neuroanatomical Features of P2 is Activity-Dependent

We demonstrate here that if OSN responses are impaired by naris occlusion there are abrupt changes in the volume and number of glomeruli and there are no longer any differences between the lateral and medial domains. Zou and co-workers (2004) showed that the number of M71 and M72 glomeruli decreased through postnatal development, and that the change in number was activity-dependent. They proposed that the absence of sensory activity perturbs glomerular maturation during a postnatal sensitive period (0 to 90 days -12 weeks -post natal). Here we show that, at least in the case of the P2 glomerulus, the number and volume are affected by sensory activity past this sensitive period (from 12 to 16 weeks of age). Interestingly, in the case of P2, naris occlusion elicits a marked decrease in the number of glomeruli while the opposite was shown for M71 and M72 by Zou and co-workers. It is unclear whether this difference is due to the different age of the mice, the fact that we studied different glomeruli or differences in cage environments between the two laboratories. What is clear is that glomerular features are highly plastic even in the adult mice, a fact that might affect odor information processing after prolonged exposure to different odor environments. Of note the volume of P2 glomeruli is affected by naris occlusion in the *contralateral* side (Figure 4) presumably because of the increased air flow in the opposite naris that would result in a change in odor exposure for the olfactory epithelium (Kimbell et. al. 1997).

Our experiments show that both naris occlusion and a decrease in gene dosage for BDNF reduce the asymmetry between lateral and medial glomeruli. Although our work does not show how these manipulations affect the volume and number of P2 glomeruli, these results do raise the question whether a mechanism can be hypothesized to explain the differential effects between medial and lateral glomeruli. Two recent manuscripts show that sensory activity of OSNs affects the location and number of glomeruli innervated by the axons from OSNs expressing the same receptor (Imai et al., 2006;Zou et al., 2007). Thus, it is reasonable to propose that the number and volume of individual glomeruli is influenced by OSN activity. As stated in the previous section, it is likely that the concentration of odor molecules detected by the P2 receptors differs between the medial and lateral glomeruli because air flow patterns differ in these areas of the OE (Kimbell et al., 1997), and because the olfactory epithelium exhibits chromatographic features (Mozell, 1970). We hypothesize that this difference in concentration of odor molecules reaching the P2 glomeruli elicits differential activity in these OSNs leading to modifications in axon targeting that result in

differences in volume and number of glomeruli between the medial and lateral domains. This hypothesis would be consistent with modification of asymmetry by sensory deprivation by naris occlusion and with the effect of BDNF on glomerular asymmetry because BDNF expression in the olfactory bulb is known to be activity-dependent (McLean et al., 2001).

Additional Information Provided by Mirror-Image Maps

Based on the data presented we speculate that the asymmetric responses of the mirror-image odor maps acts to convey additional information that would not be present if the bulb contained a single glomerular map. Thus, in the case of H-2b urine the interaction among glomerular columns is likely very different when the P2 glomeruli across the two domains are compared. Because interactions between glomerular columns are likely to play an important role in odor quality coding, the presence of asymmetries would allow the information to be processed in two different manners, thereby providing additional information. This is likely to be important for complex multicomponent odorants. Interestingly, at least at the level of *c-fos*, while the odor map elicited by H-2b urine is markedly asymmetric, the odor map elicited by H-2k urine (from mice with a different MHC haplotype) is more symmetric (Schaefer et al., 2002). It is unusual that some, and not all, complex odors such as urine elicit more asymmetric odor maps, particularly because the difference in chemical composition between H-2b and H-2k urine is thought to be in the relative concentration of specific volatile components, rather than because of the presence of different volatile chemicals in the two urines (Beauchamp and Yamazaki, 2005;Schaefer et al., 2002).

Acknowledgments

We thank Dr. Thomas Finger for help with neuroanatomical methods and discussion. This work was supported by grants from the NIH to KRJ and DR.

This work was supported by grants NIH DC00566 and DC004657 (to DR)

Reference List

Aungst JL, Heyward PM, Puche AC, Karnup SV, Hayar A, Szabo G, Shipley MT. Centre-surround inhibition among olfactory bulb glomeruli. Nature. 2003; 426:623–629. [PubMed: 14668854]

Baker H, Morel K, Stone DM, Maruniak JA. Adult naris closure profoundly reduces tyrosine hydroxylase expression in mouse olfactory bulb. Brain Res. 1993; 614:109–116. [PubMed: 8102310]

Beauchamp GK, Yamazaki K. Individual differences and the chemical senses. Chem Senses. 2005; 30 Suppl 1:i6–i9. [PubMed: 15738195]

Bennett JL, Zeiler SR, Jones KR. Patterned expression of BDNF and NT-3 in the retina and anterior segment of the developing mammalian eye. Invest Ophthalmol Vis Sci. 1999; 40:2996–3005. [PubMed: 10549663]

Buck L, Axel R. A novel multigene family may encode odorant receptors: a molecular basis for odor recognition. Cell. 1991; 65:175–187. [PubMed: 1840504]

Buck LB. Unraveling the sense of smell (Nobel lecture). Angew Chem Int Ed Engl. 2005; 44:6128–6140. [PubMed: 16175527]

Cao L, Dhilla A, Mukai J, Blazeski R, Lodovichi C, Mason CA, Gogos JA. Genetic modulation of BDNF signaling affects the outcome of axonal competition in vivo. Curr Biol. 2007; 17:911–921. [PubMed: 17493809]

Christie JM, Westbrook GL. Lateral excitation within the olfactory bulb. J Neurosci. 2006; 26:2269–2277. [PubMed: 16495454]

Clevenger AC, Salcedo E, Jones KR, Restrepo D. BDNF-Promoter Mediated â-Galactosidase Expression in the Olfactory Epithelium and Bulb. Chem Senses. 2008 In press.

Ernfors P, Lee KF, Jaenisch R. Mice lacking brain-derived neurotrophic factor develop with sensory deficits. Nature. 1994; 368:147–150. [PubMed: 8139657]

Friedrich RW, Korsching SI. Chemotopic, combinatorial, and noncombinatorial odorant representations in the olfactory bulb revealed using a voltage-sensitive axon tracer. J Neurosci. 1998; 18:9977–9988. [PubMed: 9822753]

Imai T, Suzuki M, Sakano H. Odorant receptor-derived cAMP signals direct axonal targeting. Science. 2006; 314:657–661. [PubMed: 16990513]

Johnson BA, Leon M. Chemotopic odorant coding in a mammalian olfactory system. J Comp Neurol. 2007; 503:1–34. [PubMed: 17480025]

Jones KR, Farinas I, Backus C, Reichardt LF. Targeted disruption of the BDNF gene perturbs brain and sensory neuron development but not motor neuron development. Cell. 1994; 76:989–999. [PubMed: 8137432]

Kimbell JS, Godo MN, Gross EA, Joyner DR, Richardson RB, Morgan KT. Computer simulation of inspiratory airflow in all regions of the F344 rat nasal passages. Toxicol Appl Pharmacol. 1997; 145:388–398. [PubMed: 9266813]

Levai O, Breer H, Strotmann J. Subzonal organization of olfactory sensory neurons projecting to distinct glomeruli within the mouse olfactory bulb. J Comp Neurol. 2003; 458:209–220. [PubMed: 12619077]

Lin W, Arellano J, Slotnick B, Restrepo D. Odors detected by mice deficient in cyclic nucleotide-gated channel subunit A2 stimulate the main olfactory system. J Neurosci. 2004; 24:3703–3710. [PubMed: 15071119]

Linster C, Johnson BA, Yue E, Morse A, Xu Z, Hingco EE, Choi Y, Choi M, Messiha A, Leon M. Perceptual correlates of neural representations evoked by odorant enantiomers. J Neurosci. 2001; 21:9837–9843. [PubMed: 11739591]

Lodovichi C, Belluscio L, Katz LC. Functional topography of connections linking mirror-symmetric maps in the mouse olfactory bulb. Neuron. 2003; 38:265–276. [PubMed: 12718860]

Marks CA, Cheng K, Cummings DM, Belluscio L. Activity-dependent plasticity in the olfactory intrabulbar map. J Neurosci. 2006; 26:11257–11266. [PubMed: 17079653]

McLean JH, rby-King A, Bonnell WS. Neonatal olfactory sensory deprivation decreases BDNF in the olfactory bulb of the rat. Brain Res Dev Brain Res. 2001; 128:17–24.

Mombaerts P, Wang F, Dulac C, Chao SK, Nemes A, Mendelsohn M, Edmondson J, Axel R. Visualizing an olfactory sensory map. Cell. 1996; 87:675–686. [PubMed: 8929536]

Mori K, Takahashi YK, Igarashi KM, Yamaguchi M. Maps of odorant molecular features in the Mammalian olfactory bulb. Physiol Rev. 2006; 86:409–433. [PubMed: 16601265]

Mozell MM. Evidence for a chromatographic model of olfaction. J Gen Physiol. 1970; 56:46–63. [PubMed: 5514160]

Nagao H, Yoshihara Y, Mitsui S, Fujisawa H, Mori K. Two mirror-image sensory maps with domain organization in the mouse main olfactory bulb. Neuroreport. 2000; 11:3023–3027. [PubMed: 11006987]

Rinberg D, Koulakov A, Gelperin A. Speed-accuracy tradeoff in olfaction. Neuron. 2006; 51:351–358. [PubMed: 16880129]

Royet JP, Souchier C, Jourdan F, Ploye H. Morphometric study of the glomerular population in the mouse olfactory bulb: numerical density and size distribution along the rostrocaudal axis. J Comp Neurol. 1988; 270:559–568. [PubMed: 3372747]

Rubin BD, Katz LC. Optical imaging of odorant representations in the mammalian olfactory bulb. Neuron. 1999; 23:499–511. [PubMed: 10433262]

Salcedo E, Zhang C, Kronberg E, Restrepo D. Analysis of training-induced changes in ethyl acetate odor maps using a new computational tool to map the glomerular layer of the olfactory bulb. Chem Senses. 2005; 30:615–626. [PubMed: 16141292]

Schaefer ML, Finger TE, Restrepo D. Variability of position of the P2 glomerulus within a map of the mouse olfactory bulb. J Comp Neurol. 2001; 436:351–362. [PubMed: 11438935]

Schaefer ML, Yamazaki K, Osada K, Restrepo D, Beauchamp GK. Olfactory fingerprints for major histocompatibility complex-determined body odors II: relationship among odor maps, genetics, odor composition, and behavior. J Neurosci. 2002; 22:9513–9521. [PubMed: 12417675]

Schoppa NE. A novel local circuit in the olfactory bulb involving an old short-axon cell. Neuron. 2006; 49:783–784. [PubMed: 16543124]

Schoppa NE, Westbrook GL. Glomerulus-specific synchronization of mitral cells in the olfactory bulb. Neuron. 2001; 31:639–651. [PubMed: 11545722]

Sharp FR, Kauer JS, Shepherd GM. Laminar analysis of 2-deoxyglucose uptake in olfactory bulb and olfactory cortex of rabbit and rat. J Neurophysiol. 1977; 40:800–813. [PubMed: 886371]

Shepherd, GM.; Chen, WR.; Greer, CA. The Synaptic Organization of the Brain. New York: Oxford University Press; 2004.

Spors H, Wachowiak M, Cohen LB, Friedrich RW. Temporal dynamics and latency patterns of receptor neuron input to the olfactory bulb. J Neurosci. 2006; 26:1247–1259. [PubMed: 16436612]

Tisay KT, Bartlett PF, Key B. Primary olfactory axons form ectopic glomeruli in mice lacking p75NTR. J Comp Neurol. 2000; 428:656–670. [PubMed: 11077419]

Treloar HB, Feinstein P, Mombaerts P, Greer CA. Specificity of glomerular targeting by olfactory sensory axons. J Neurosci. 2002; 22:2469–2477. [PubMed: 11923411]

Uchida N, Mainen ZF. Speed and accuracy of olfactory discrimination in the rat. Nat Neurosci. 2003; 6:1224–1229. [PubMed: 14566341]

Wachowiak M, Cohen LB. Representation of odorants by receptor neuron input to the mouse olfactory bulb. Neuron. 2001; 32:723–735. [PubMed: 11719211]

Willhite DC, Nguyen KT, Masurkar AV, Greer CA, Shepherd GM, Chen WR. Viral tracing identifies distributed columnar organization in the olfactory bulb. Proc Natl Acad Sci U S A. 2006; 103:12592–12597. [PubMed: 16895993]

Xu F, Greer CA, Shepherd GM. Odor maps in the olfactory bulb. J Comp Neurol. 2000; 422:489–495. [PubMed: 10861521]

Zou DJ, Chesler AT, Le Pichon CE, Kuznetsov A, Pei X, Hwang EL, Firestein S. Absence of adenylyl cyclase 3 perturbs peripheral olfactory projections in mice. J Neurosci. 2007; 27:6675–6683. [PubMed: 17581954]

Zou DJ, Feinstein P, Rivers AL, Mathews GA, Kim A, Greer CA, Mombaerts P, Firestein S. Postnatal refinement of peripheral olfactory projections. Science. 304:1976–1979.

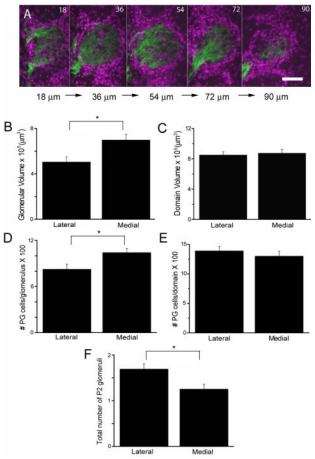

Figure 1. Asymmetric neuroanatomical features of P2 glomeruli

A, shows fluorescent micrographs of serial sections through a single P2 glomerulus (tauGFP is shown in green) with surrounding JG cells (magenta). B–F. Bar graphs comparing: lateral and medial P2 glomerular volume (**B**), lateral and medial P2 domain volume (**C**), the total number of JG cells surrounding the lateral and medial P2 glomeruli (**D**), the total number of JG cells in the lateral and medial P2 domains (**E**), and the number of P2 glomeruli on the lateral and medial aspects of the MOB (**F**). Data were from 10 animals. Scale bar 50 µm.

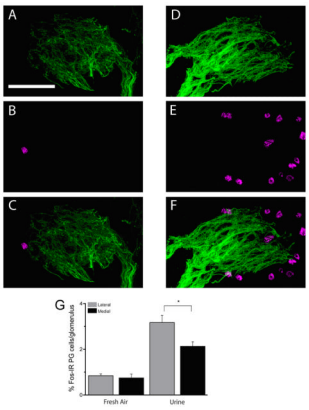

Figure 2.

A–C, shows fluorescent micrographs of a single section through a single P2 glomerulus (tauGFP is displayed green) with surrounding JG cells that have Fos-like IR (magenta) in a mouse exposed to fresh air. **D–F**, show fluorescent micrographs of a single section through a single P2 glomerulus (green) with surrounding JG cells that have Fos-like IR (magenta) in a mouse exposed to urine. G. Bar graph comparing the percentage of Fos-like IR JG cells surrounding the lateral and medial P2 glomeruli in mice exposed to fresh air and urine. Data were from 4 animals for fresh air and 6 animals for urine. Scale bar 50 μm.

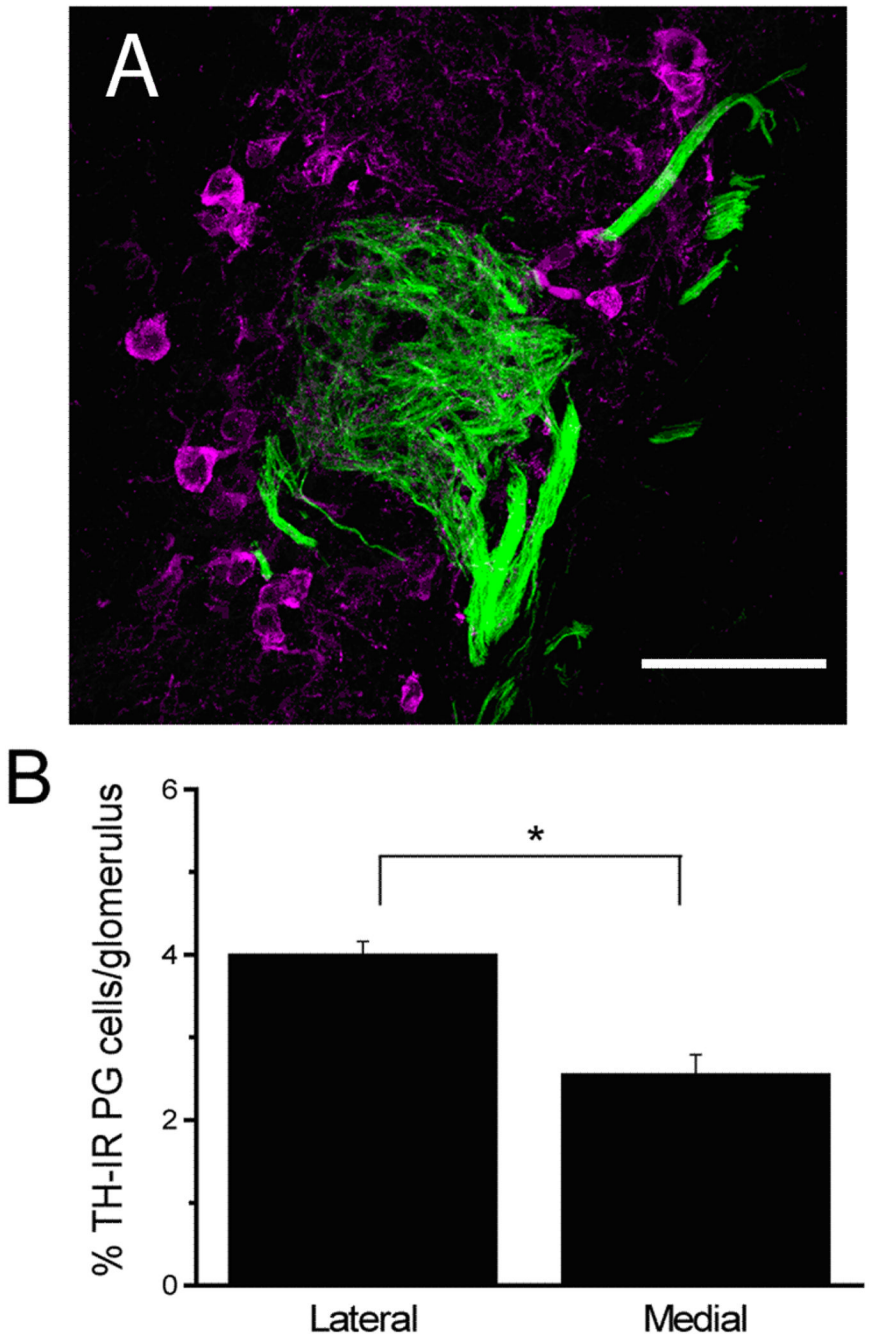

Figure 3. Differential expression of TH between the lateral and medial P2 domains

A, representative fluorescence micrograph of TH-IR JG cells (magenta) surrounding a P2 glomerulus (green). **B**. Bar graph of the total number of TH-IR JG cells per P2 glomerulus (Mean +/−SE). Data were from 7 animals. Scale bar 50 μm.

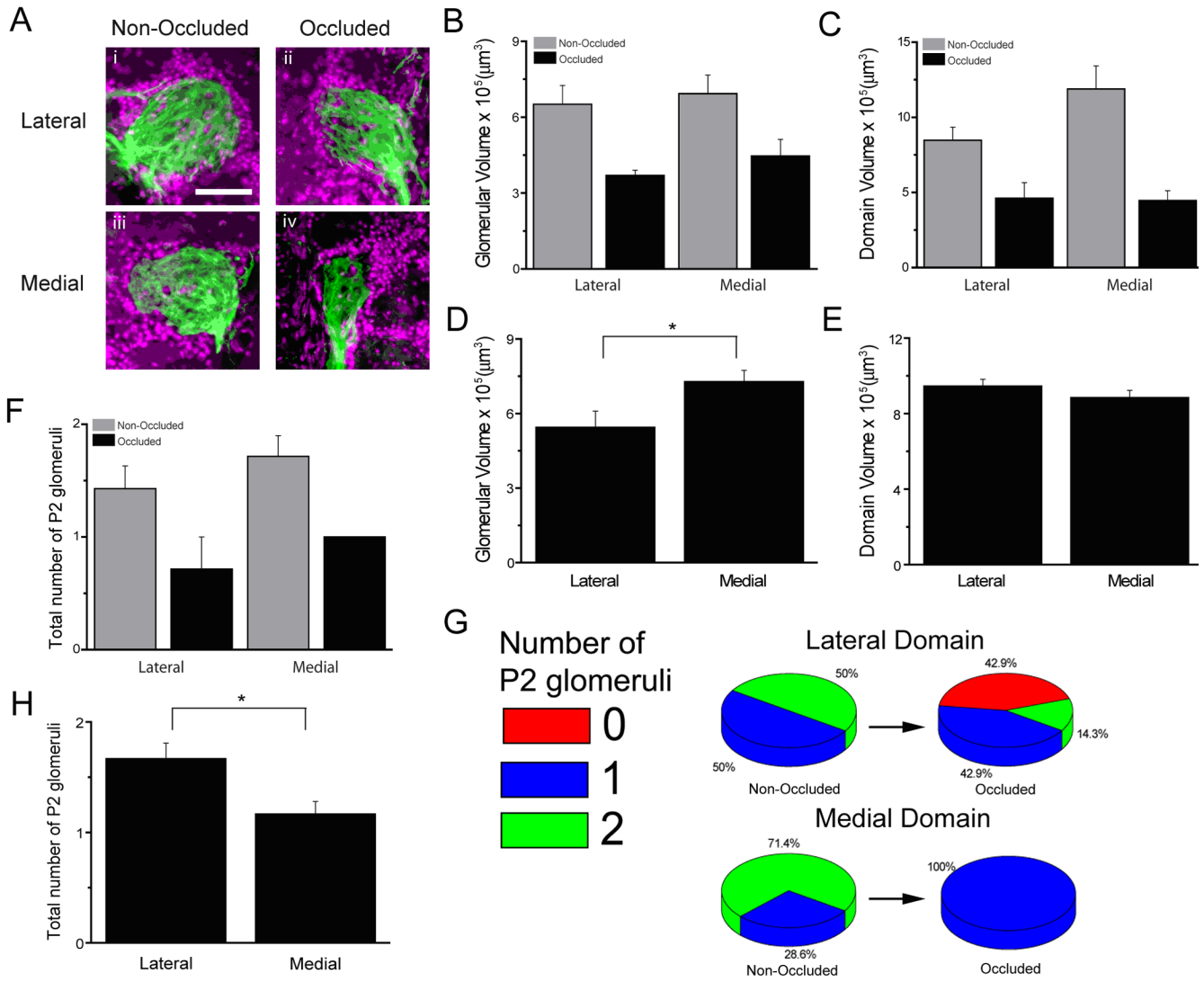

Figure 4. Neuroanatomical features of P2 glomeruli in mice with naris occlusion and sham surgery

A, representative fluorescent micrographs of P2 glomeruli from the lateral and medial domains in ipsilateral and contralateral bulbs from mice with naris occlusion. Bar graphs showing P2 glomerular volume in occluded and non-occluded bulbs (**B**), P2 domain volume in occluded and non-occluded bulbs (**C**), P2 glomerular volume in sham surgery mice (**D**), P2 domain volume in sham surgery mice (**E**), the total number of glomeruli in occluded and non-occluded mice (**F**), and the total number of glomeruli in sham surgery mice (**H**). **G**, pie graphs showing the number of glomeruli in the lateral and medial domains of occluded and non-occluded bulbs. Data were from 7 animals for naris occlusion and 6 animals for sham surgery. Scale bar 50 µm.

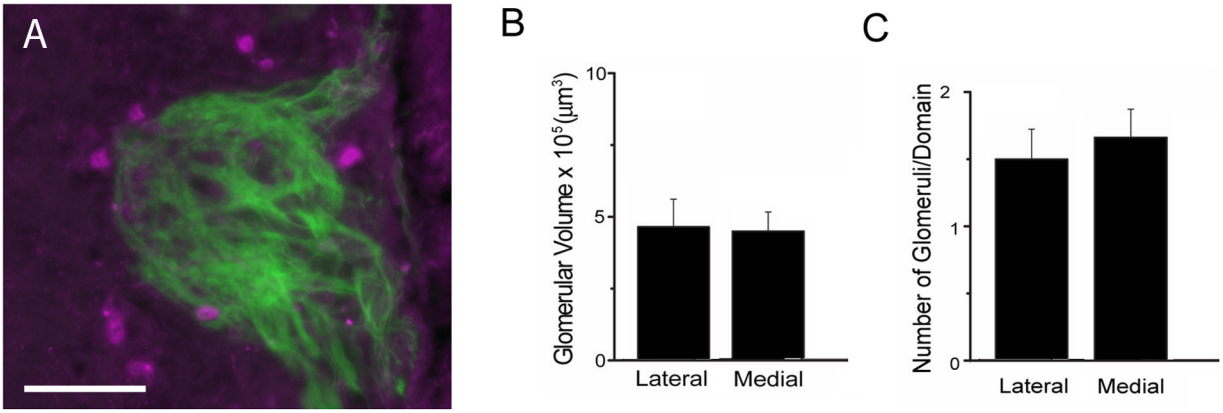

Figure 5. Reduction in BDNF gene copy number results in abolishion of asymmetry in glomerular volume and number

A. Confocal image of a P2 glomerulus from P2-IRES-tauGFP mice where one of the BDNF alleles has been replaced by an allele where the coding region of BDNF is replaced by DNA encoding for LacZ. Green: tauGFP signal in the axon terminals of the P2 OSNs. Magenta: LacZ expression in juxtaglomerular cells. **B and C.** Glomerular volume (**B**) and number of glomeruli per domain (**C**) for the lateral and medial domains of the glomerular map. Data were from 8 animals. Scale bar 50 μm.